journal

J. Am. Ceram. Soc., **81** [6] 1477–86 (1998)

Synthesis of Ultrafine β″-Alumina Powders via Flame Spray Pyrolysis of Polymeric Precursors

Anthony C. Sutorik, Siew Siang Neo,* David R. Treadwell,* and Richard M. Laine*

Departments of Materials Science and Engineering, and Chemistry,
Macromolecular Science and Engineering Center, University of Michigan, Ann Arbor, Michigan 48109–2136

Flame spray pyrolysis of a polymeric precursor is used to prepare ultrafine powders that, when sintered, convert to essentially pure phase lithium-doped sodium β″-alumina. The precursor $Na_{1.67}Al_{10.67}Li_{0.33}[N(CH_2CH_2O)_3]_{10.67}$-$[OCH_2CH_2O]\cdot x(HOCH_2CH_2OH)$ has been synthesized from stoichiometric amounts of metal hydroxides and triethanolamine ($N(CH_2CH_2OH)_3$, TEA) in excess ethylene glycol. The precursor is dissolved in ethanol, and an atomized spray of the solution is combusted in a specially constructed flame spray apparatus. Combustion occurs at ~2000°C, followed by immediate quenching. This procedure provides for a measure of kinetic control over the process. The resulting nanopowder particles are 50–150 nm in diameter and exhibit powder X-ray diffractometry patterns similar to β″-alumina. Heating the nanopowder at 30°C/min to 1200°C with a 1 h isotherm converts it to pure β″-alumina. In preliminary sintering studies, green powder compacts (~65% theoretical density) sintered at 1600°C for 12 min densify to 3.0 ± 0.1 g/cm³ (~92% theoretical density) with minimal loss of Na_2O. This procedure offers several processing and cost advantages over conventional β″-alumina syntheses.

I. Introduction

The materials β- and β″-alumina ($Na_2O\cdot xAl_2O_3$) are high-temperature solid electrolytes that exhibit high ionic conductivity as Na^+ ions migrate (~800°C) through a surplus of cationic sites in the crystal lattice.[1] These materials have been used in energy storage,[2] alkali-metal thermal-to-electric conversion (AMTEC) cells,[3] and gas sensors.[4] The high mobility of Na^+ ions also permits substantial ion-exchange chemistry.[5] β″-alumina is particularly amenable to the exchange of Na^+ ions with other monovalent, as well as divalent and trivalent, metal cations. The resulting materials have applications as optical materials[6] and photoluminescents.[7] Despite extensive study, synthesis and processing difficulties have limited the commercialization of these materials.

Many of the challenges in working with β- and β″-alumina result from the desire to optimize the formation of β″-alumina (which has the higher ionic conductivity) over that of β-alumina. The structures of β- and β″-alumina are closely related polytypes; both have the same general stacking pattern of Al–O spinel-like blocks separated by Na–O planes.[8] β-alumina is distinguished by having the interlayer Na–O lying on a crystallographic mirror plane and two Al–O blocks per unit cell. β″-alumina, rather, has a three-fold screw axis perpendicular to the planes and consequently possesses three Al–O blocks in its unit cell. The structural differences are accompanied by compositional variations. Both phases are stable over a range of sodium contents. In general, however, β-alumina is favored at lower sodium levels (idealized formula: $NaAl_{11}O_{17}$) and β″-alumina, at higher sodium levels (idealized formula: $NaAl_5O_8$).

Synthesizing β″-alumina preferentially over β-alumina using solid-state reactions is not straightforward, because of inherent atomic-scale inhomogeneity in starting material mixtures and diffusion limitations. Mixtures of the two polytypes commonly result. An additional complication is that, in simple Na/Al/O systems, β-alumina is the more thermodynamically stable of the two; β″-alumina typically forms at ~1100°C but disproportionates to β-alumina and sodium aluminate ($NaAlO_2$) at 1550°C.[9] When a portion of the Al^{3+} ions is substituted with a lower-valency metal ion (commonly Li^+ or Mg^{2+}), an increased amount of Na^+ ions is required to charge balance the anionic spinel blocks, increasing the thermodynamic stability of β″-alumina.[10] The optimum dopant levels represent only a small portion of the total reaction mixture (8 wt% Na_2O + 2 wt% MgO;[10a] 8.9 wt% Na_2O + 0.7 wt% Li_2O[10c]). Thus, starting solids must be thoroughly mixed to achieve maximum homogeneity, i.e., by ball milling and spray drying.

In recent years, judicious choice of aluminum-containing starting material has led to many successful syntheses of β″-alumina.[11] Procedures have been patented using transition-alumina phases (i.e., γ-alumina),[11a] aluminum hydroxides (i.e., bayerite, $Al(OH)_3$),[11b] and aluminum oxyhydroxides (i.e., boehmite, γ-AlOOH).[11c,d,e] These starting materials have structures (or convert to structures when dehydrated) with a spinel-like Al–O network similar to that found in the β-alumina polytypes. As such, the overall reaction now requires less energy, resulting in a thermodynamic shortcut that favors β″-alumina formation.[11e]

However, successful formation of β″-alumina is only part of the problem. Next, the ceramic powders must be processed into useful shapes. This operation requires sintering compacted powders at temperatures (1500°–1600°C) well above the soda (Na_2O) sublimation temperature (1275°C).[12] Recall that β-alumina is the polytype favored at lower sodium ratios. This observation is true even when the stabilizing dopants are present; thus, as sintering progresses, Na_2O sublimation from between the layers drives the conversion of β″-alumina to β-alumina. Several processing tricks can be used to minimize Na_2O loss (i.e., packing the green bodies in Na_2O-rich material or using sealed and inert reaction vessels), each of which increases the complexity and cost of processing.[2b]

Given these synthetic and processing complexities, commercial production of β″-alumina ceramic bodies is a substantial undertaking. Only one U.S. manufacturer, Ceramatec (Salt Lake City, UT), has been engaged in the manufacture of β″-alumina components, and it has recently stopped production. Despite almost thirty years of research and development, the need still exists for an easy, inexpensive, and reliable way to synthesize and process β″-alumina.

B. Dunn—contributing editor

Manuscript No. 191329. Received December 16, 1996; approved August 26, 1997.
Supported through a cooperative agreement with Advanced Modular Power Systems (Ann Arbor, MI), under a NASA STTR Phase II grant (No. F49620-97-C-0006).
*Member, American Ceramic Society.

As part of a program to develop facile techniques for the synthesis and processing of metal oxide nanopowders, several new methods have been developed. First, new metal alkoxide precursors were synthesized based on a one-pot dissolution of metal hydroxides or oxides in ethylene glycol made basic with triethanolamine.[13] These precursors provide for stable atomic-scale mixing of the component metals. Second, when atomized and combusted in a flame spray pyrolysis apparatus (~2000°C), ethanolic solutions of these precursors have yielded nanosized particles of the target oxide.[14] Because these particles possess high surface energy, they should sinter to dense bodies at lower temperatures than those required for larger-sized, conventional powders.[15] Also, the pyrolysis technique exposes the precursor and resultant oxide nanopowders to high temperatures for only a few seconds during the initial combustion, which is followed by immediate, rapid cooling. This approach should access kinetically stable oxides, a feature associated with neither traditional solid-state reactions nor conventional bulk precursor pyrolysis. By combining the benefits of simple polymeric precursor synthesis and flame spray pyrolysis, high-purity lithium-doped β″-alumina (composition: $Na_{1.67}Al_{10.67}Li_{0.33}O_{17}$) can be easily synthesized. The present report details this work, along with initial studies on the nanopowder processability. A more detailed study of compaction, sintering, and densification of the β″-alumina nanopowders to monolithic shapes, and their resulting properties, is in progress.[16]

II. Experimental Procedure

(1) Synthetic Procedure

(A) Reagents: All materials were used as received from their commercial sources: NaOH, Mallinckrodt, Paris, KY; $LiOH{\cdot}H_2O$, Strem Chemical, Newburyport, MA; $Al(OH)_3{\cdot}xH_2O$, Aldrich Chemical Co., Milwaukee, WI; triethanolamine, $N(CH_2CH_2OH)_3$ (TEA), 98%, Aldrich Chemical Co.; and ethylene glycol, $HOCH_2CH_2OH$, (EG), reagent grade, J. T. Baker, Phillipsburg, NJ. All materials were handled in air except where noted. The water content of each batch of $Al(OH)_3{\cdot}xH_2O$ was determined by thermal gravimetric analysis (TGA). Ethylene glycol was recycled by redistilling twice; therefore, the supply used was either redistilled or freshly received.

For comparison purposes, a sample of precursor powder and a finished β″-alumina ceramic tube were obtained from Ceramatec. The components of the precursor powder remain unknown; however, the identity of the ceramic was confirmed by powder X-ray diffractometry (XRD).

(B) Synthesis of Precursor 1, $Na_{1.67}Al_{10.67}Li_{0.33}(TEA)_{10.67}{\cdot}x(EG)$: In a 2 L round-bottom flask, 199.9 g (2.190 mol) of $Al(OH)_3{\cdot}0.72H_2O$, 326.7 g (2.190 mol) of TEA, and 1 L of EG are mixed with constant stirring (magnetic). The reaction is heated to ~200°C to distill off EG and byproduct water. After ~2 h, the reaction turns clear, indicating that formation of a soluble $[Al(TEA)]_x$ complex is complete. Then, 13.71 g (0.343 mol) of NaOH and 2.84 g (0.068 mol) of $LiOH{\cdot}H_2O$ are added, and the reaction is refluxed for 1 h. The metal molar ratio used (Na:Al:Li = 1.67:10.67:0.33) represents the previously determined optimum doping level,[10c] which is also used in commercially available Ceramatec β″-alumina ceramic tubes. The reaction is then distilled under N_2, first to remove byproduct water then excess EG, until the residue is too viscous to stir. On cooling, a glassy, orange/yellow solid is recovered from the flask and stored in air. Yields are essentially quantitative.

Rigorous characterization (TGA, ^{27}Al NMR and ^{13}C NMR (nuclear magnetic resonance) spectroscopy, fast atom bombardment mass spectroscopy (FAB-MS), and infrared (IR) spectroscopy) was performed on samples dried under vacuum for an additional 4–8 h (180°C). To investigate the effect of changes in elemental composition on the products of flame pyrolysis, the above procedure was also used to synthesize precursors with Na:Al:Li metal ratios of 1.90:10.67:0.33 (precursor 2) and 1.90:10.55:0.45 (precursor 3).

(C) Synthesis of Flame-Spray-Pyrolyzed Nanopowder, $Na_{1.67}Al_{10.67}Li_{0.33}O_{17}$: A more detailed description of the general procedure for nanopowder formation has been published.[14] A schematic of the apparatus used is given in Fig. 1. For combustion in the flame spray apparatus, the polymer is dissolved in anhydrous ethanol. Typically, 10–20 wt% solutions are prepared, because they give the appropriate viscosity for use in the apparatus. During flame spray pyrolysis, the precursor solution is fed into the pyrolysis chamber of the device. The solution is atomized to an aerosol and ignited via natural-gas/oxygen pilot torches. Combustion occurs at ~2000°C, instantly converting the precursor to an ultrafine oxide powder. Cooling of the nanopowder begins immediately as it is swept away from the combustion zone by the natural flow of gases. The nanopowders are collected downstream in a series of electrostatic precipitation (ESP) tubes charged with a 10 kV dc bias. After the run is complete, powders are manually brushed from the ESP tubes and stored in a vacuum desiccator. Analysis is performed using XRD and IR spectroscopy.

(D) Sintering of Flame-Spray-Pyrolyzed Nanopowder: The sintering behavior of the nanopowders was initially investigated using compacted green disks formed from (i) as-prepared

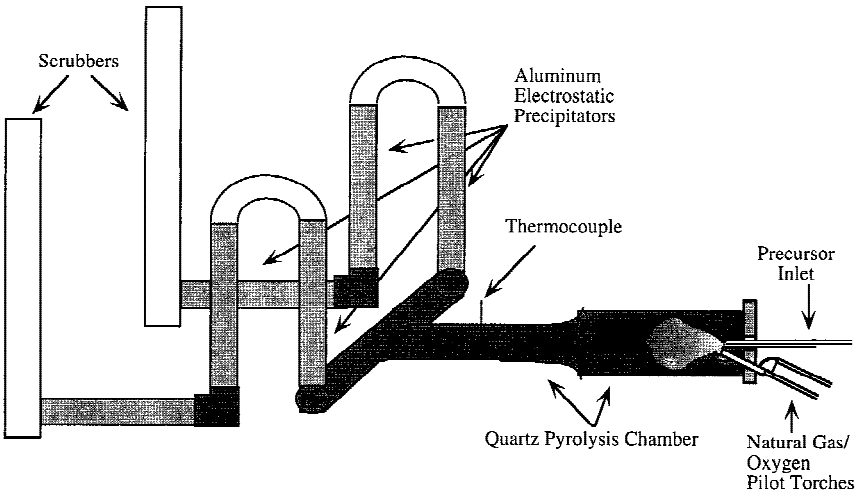

Fig. 1. Schematic of the flame-spray-pyrolysis apparatus.

nanopowders and (ii) powders mixed with 10–20 wt% of the initial precursor as binder. Powder/binder mixtures were prepared by dissolving the desired amount of polymer in a minimum of anhydrous ethanol. The nanopowder was then added, and the sides of the beaker were rinsed with enough ethanol to cover the powder. The slurry was sonicated (Model 1200, Branson, Danbury, CT) until the solvent evaporated completely (2–4 h). The solid residue was dried in a drying oven for 1–2 h and ground to a fine powder with a mortar and pestle.

Pellets were formed by loading 250–350 mg of the desired powder into a stainless-steel, double-action die (1.275 cm in diameter) and pressing the assembled device in a laboratory press, (Model 3912, Fred S. Carver, Menomonee Falls, WI). Pressures of either 25 or 52 ksi (~170 or 360 MPa, respectively) were applied and held for ~5 min. The formed pellets (1.275 cm diameter × 0.2 cm) were then carefully ejected from the die and sintered in a box furnace (Model No. 58114, Linberg/Blue, Watertown, WI) equipped with a microprocessor (Model No. 818 P, Eurotherm, Northing, U.K.). Alumina boats were used for the sintering studies. To guard against excess sodium volatilization, the pellets were packed in a powder formed from the pyrolysis of sodium and aluminum formates in a 1:2 ratio.[†] Samples made from as-prepared nanopowder were heated at a rate of 30°C/min to the desired sintering temperature. For pellets that contained binder, the heating rate was 1°C/min to 500°C, to ensure slow burnout of the organic components. Heating rates to the sintering temperature were then 30°C/min, as used previously. The cooling rate for all samples was 50°C/min.

(2) Instrumental Methods

(A) Thermal Gravimetric Analysis (TGA): Thermal analyses were performed (Model Thermal Analyst 2200 with a Hi-Res TGA 2950 thermogravimetric analyzer, TA Instruments, New Castle, DE). TGA samples, 10–20 mg in platinum pans, were heated using the Hi-Res™ ramp-rate program, which decreases the heating rate as the rate of mass loss increases, to provide sharply defined thermal events. The TGA balance flow meter was set at 40 cm^3/min N_2, whereas the purge flow meter was adjusted to 60 cm^3/min of synthetic air.

(B) Differential Thermal Analysis (DTA): These analyses were performed on a Thermal Analyst 2200 apparatus (with a differential scanning calorimeter module (Model DSC 2910, TA Instruments) equipped with a differential thermal analyzer (Model 1600 DTA, TA Instruments)). DTA samples, 20–25 mg, were loaded into platinum crucibles and heated at a rate of 20°C/min. The DTA purge flow meter was adjusted to 50 cm^3/min of synthetic air. Calcined alumina (Aluminum Co. of America, Pittsburgh, PA) was used as a reference.

(C) Powder X-ray Diffractometry (XRD): Samples were analyzed using a double-crystal wide-angle goniometer (Model 2θ, Rigaku Co., Tokyo, Japan). Specimens (0.05–0.2 g) were ground with an alumina mortar and pestle, packed in a glass specimen holder, and placed in the diffractometer. Scans were measured from 5°–80° 2θ at a scan speed of 5° 2θ/min in 0.05° or 0.03° 2θ increments using Cu*K*α radiation (40 kV, 100 A). Peak positions were compared with standard JCPDS[‡] files to identify crystalline phases.

(D) Diffuse Reflectance Infrared Transmission Spectroscopy (DRIFTS): DRIFTS spectra were obtained on a Galaxy Series 3020 bench spectrometer (Mattson Instruments, Madison, WI) adapted with a ''Praying Mantis'' diffuse reflectance accessory (Model DRA-2CO, Harrick Scientific, Ossining, NY). The system was continuously purged with liquid nitrogen boil-off. Single-crystal potassium bromide (KBr, International Crystal Labs, Garfield, NJ), powdered with an alumina mortar and pestle, was used as the nonabsorbing medium. Samples were prepared using 0.3–0.5 wt% of analyte rigorously mixed with the powdered KBr.

(E) Nuclear Magnetic Resonance (NMR): Samples of polymeric precursor were dissolved in either deuterated or nondeuterated chloroform to form an ~10 wt% solution. NMR spectra were recorded using a 360 MHz spectrometer (Bruker Instruments, Billerica, MA). ^{27}Al NMR spectra were obtained with the spectrometer operating at 93.8 MHz and using a 41000 Hz spectral width, a relaxation delay of 0.2 s, and a pulse width of 13°. Deuterium oxide (D_2O) in a sealed inner tube served as the lock solvent, and a 1*M* solution of $AlCl_3$ in D_2O:H_2O (1:1) served as the external reference. ^{13}C NMR spectra were obtained with the spectrometer operating at 90.5 MHz and using a 20000 Hz spectral width, a relaxation delay of 0.2 s, and a pulse width of 4.1°.

(F) Fast Atom Bombardment Mass Spectroscopy (FAB-MS): Mass spectra of the samples were recorded (Model 7070E, Fisons Instruments, Beverly, CA) at the Department of Chemistry at The University of Michigan. The samples were dissolved in dry dichloromethane (CH_2Cl_2) and dispersed in a matrix of *p*-nitrobenzylalcohol (NBA). Analyses were performed in positive ion mode.

(G) Scanning Electron Microscopy (SEM): The grain structure of sintered compacts of nanopowders was examined using an SEM microscope (Model S800, Hitachi, Tokyo, Japan) operating at 5 keV. SEM samples were mounted on an aluminum stub using carbon paste and sputter coated with ~0.1 μm gold/palladium to improve conductivity.

(H) Transmission Electron Microscopy (TEM): For TEM (Model 420 TM, Philips Electronic Instruments, Mahwah, NJ) characterization, nanopowders were suspended in isopropanol, ultrasonicated, and pipetted onto a holey carbon grid (SPI Industries, Indianapolis, IN). After the isopropanol evaporated, the samples were imaged without further preparation.

(I) Sintering: A Type 6000 box furnace (Thermolyne, Dubuque, IA) was used for the sintering experiments at ≤1000°C, and the previously described Linberg/Blue box furnace was used at ≥1200°C. Alumina boats that had been prereacted with sodium carbonate (Na_2CO_3) were used as sample containers. Heating and cooling rates were 30°C/min and 50°C/min, respectively, unless otherwise noted.

III. Results and Discussion

(1) Precursor Synthesis Characterization

The one-pot synthesis process that has been used leads to a highly stable polymer-like precursor in an ethylene glycol solution.[13] No precipitate forms as the solution is concentrated, which indicates that all the component metals remain dissolved and, hence, intimately mixed. This property is essential for subsequent flame spray pyrolysis because it minimizes phase separation, which ensures that the final ceramic composition mirrors that of the precursor. This ability permits ceramic compositions to be tailored simply by choosing the initial metal ratios. Following the removal of excess solvent, a hard glassy solid forms that seems to be indefinitely stable and can be stored in air. In dilute EG solutions, however, precipitates can form after standing in air for several days. These are easily redissolved by heating or distilling the solution briefly.

By using the previously optimized stoichiometry of Na:Al:Li = 1.67:10.67:0.33,[10c] precursor 1 is expected to provide high-quality lithium-doped β″-alumina. As such, it is the most extensively characterized of the precursors studied and serves

[†]The pellets were packed in a powder made from sodium and aluminum formates (Na:Al ≅ 1:2 molar ratio). $Al(O_2CH)_3$ (10.08 g (62.2 mmol) was dissolved in rapidly boiling deionized water; 2.298 g (33.8 mmol) of $Na(O_2CH)$ was added, and boiling continued until dryness. The white residue was collected, ground with a mortar and pestle, and heated at 800°C for 5 h. The material was stored in air. This material is preferred because it is less likely to fuse to the surface of the green ceramic bodies during sintering, unlike powders made by mixing aluminum and sodium precursors mechanically.

[‡]Joint Committee on Powder Diffraction Standards, Swarthmore, PA (now International Centre for Diffraction Data (ICDD), Newtowne Square, PA).

as the baseline system. The general physical and chemical characteristics of the precursors are expected to be similar, despite the slight compositional variations.

Figure 2 shows the TGA profile of a finely ground sample of precursor 1, vacuum dried for 8 h at a temperature of 180°C. The initial mass loss of 1.5% at temperatures <80°C is attributed to a small amount of moisture absorbed during sample preparation. The precursor is slightly hygroscopic when finely ground. The major mass loss begins at ~310°C, and the steepest change occurs at ~370°C. This mass loss is associated with organic ligand decomposition.[17,18] The major fraction of the decomposition products are lost as gases; however, a small fraction chars. Hence, a second major mass loss is observed in the temperature range of 370°–600°C as this char oxidizes.[19] A final ceramic yield of 29.2% is observed; however, if surface moisture is disregarded, the corrected yield is 30.7%. This value corresponds to that of a precursor with the formula $[Na_{1.67}Li_{0.33}(OCH_2CH_2O)][Al(TEA)]_{10.67}$, which has a calculated ceramic yield of 30.8%. Note that only sufficient deprotonated EG to balance the alkali-cations charge once the precursor is fully dry is present.

NMR analyses confirm that EG and TEA were the sole components of precursor 1. The ^{27}Al NMR spectrum revealed two signals, at 61.7 ppm and 5.58 ppm, which are characteristic of pentacoordinated and hexacoordinated aluminum, respectively.[20] Although chemical shifts do not correlate well to the environment in ^{27}Al NMR, the peak positions were the same as those found in studies of $[Al(TEA)]_4$.[20] ^{13}C NMR shows a weak peak at 63.6 ppm (corresponding to the EG carbon atoms) and two broad peaks, at 57.1 and 53.0 ppm (attributed to the two distinct carbons in TEA).[20,21]

Positive-ion FAB-MS analysis of precursor 1 also confirms the presence of $[Al(TEA)]_n$ species. The spectrum is dominated by peaks separated by the mass of the [Al(TEA)] monomer (173). The major series consists of peaks with *m/z* values of 174 (19% intensity), 347 (47%), 520 (10%), and 693 (9%), corresponding to oligomers $[Al(TEA)]_n$, where $n = 1$–4, plus an extra proton for the positive charge. The 100% intensity peak occurs at $m/z = 176$ and corresponds to the association of a sodium ion ($m/z = 23$) with a nitrobenzylalcohol molecule ($m/z = 153$) from the matrix. From the FAB-MS analysis, the precursor is dominated by [Al(TEA)] oligomers, with smaller amounts of lithium, sodium, and EG complexed species being more difficult to distinguish by this method.

The DRIFTS spectrum of precursor 1 is shown in Fig. 3. Several peaks characteristic of the organic component are present: ν(C–H) vibrations, centered at 2860 cm^{-1}; a collection of bands in the ν(C−O) and ν(C−N) region, at 900, 1110, and 1270 cm^{-1}; and ν(C−H) bending vibrations, at 1364 and 1450 cm^{-1}. The strong peak at ~670 cm^{-1} is likely due to ν(Al–O) vibrations. A weak, broad ν(O–H) band is centered at 3500 cm^{-1}. This peak likely originates from moisture adsorbed from the atmosphere during sample preparation.

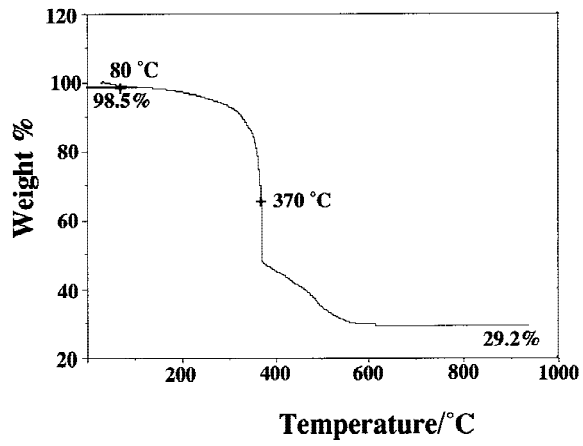

Fig. 2. TGA of precursor 1, $Na_{1.67}Al_{10.67}Li_{0.33}(TEA)_{10.67}(EG)$.

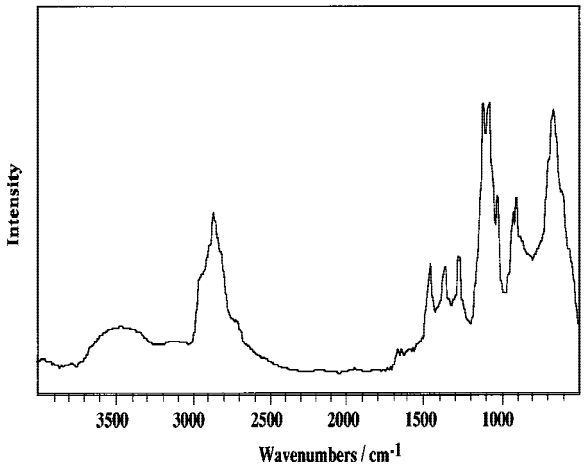

Fig. 3. DRIFTS spectrum of vacuum-dried $Na_{1.67}Al_{10.67}Li_{0.33}(TEA)_{10.67}(EG)\cdot x$EG (180°C/4 h).

Prior to the flame-spray-pyrolysis studies discussed below, bulk precursor pyrolysis studies were performed to determine the likelihood of forming β″-alumina. The heating schedules and temperatures used were based on the TGA profile. The XRD analyses of precursor 1 heated to various temperatures are shown in Fig. 4. At 500°C, the light-gray powders were X-ray amorphous. Broad peaks appeared after heating for 2 h at 1000°C. Additional heating at 1100°C for 2 h converted the material directly to β-alumina (JCPDS File No. 32-1033). No peaks characteristic of β″-alumina were observed (JCPDS File No. 19-1173). Heating the material at 1400°C for 1 h caused an increase in crystallinity, as indicated by peak sharpening and increased intensities; however β″-alumina remained absent. Mixtures of the two phases formed, using a variety of heating schedules and with trial batches of precursors of varying compositions; however, phase-pure β″-alumina was never observed. The best ratio obtained was only a 2:1 β:β″.[§]

(2) Nanopowder Characterization

The powder XRD pattern of the nanopowder synthesized from the flame spray pyrolysis of precursor 1 (pattern (a) in Fig. 5) exhibits significant crystallinity. Most of the peaks can be assigned to β″-alumina. One major exception occurs at 25.2° 2θ (3.54 Å). The origin of this peak remains unclear. It is close to the (210) peak (25.7° 2θ, 3.46 Å) of m-alumina, a sodium aluminate often observed as an intermediate in the synthesis of β-/β″-alumina;[22] however, no other distinguishing peaks from m-alumina are present. Another unassigned peak occurs at ~50° 2θ (1.82 Å); this peak is weak and, by itself, could indicate several possible aluminate byproducts. Both of these unknown peaks are present in the pattern of $LiAl_5O_8$ (JCPDS File No. 17-573); however, a definite assignment cannot be made, because of the absence of several other peaks. The peaks at 18.7° 2θ (4.75 Å), 45.9° 2θ (1.98 Å), and 66.9° 2θ (1.40 Å) are disproportionately intense, relative to the other β″-alumina peaks. Their reported intensities (JCPDS File No. 19-1173) are <5%, 80%, and 70%, respectively, whereas in the as-processed nanopowder, they are 71%, 100%, and 91%. This observation

[§]This ratio was achieved via bulk pyrolysis of a precursor, $Na_{1.67}Al_{10.67}Li_{0.33}(TEA)_{8.67}\cdot x$EG. The heating schedule used was 375°C/2 h, 800°C/8 h, and 1500°C/12 min.

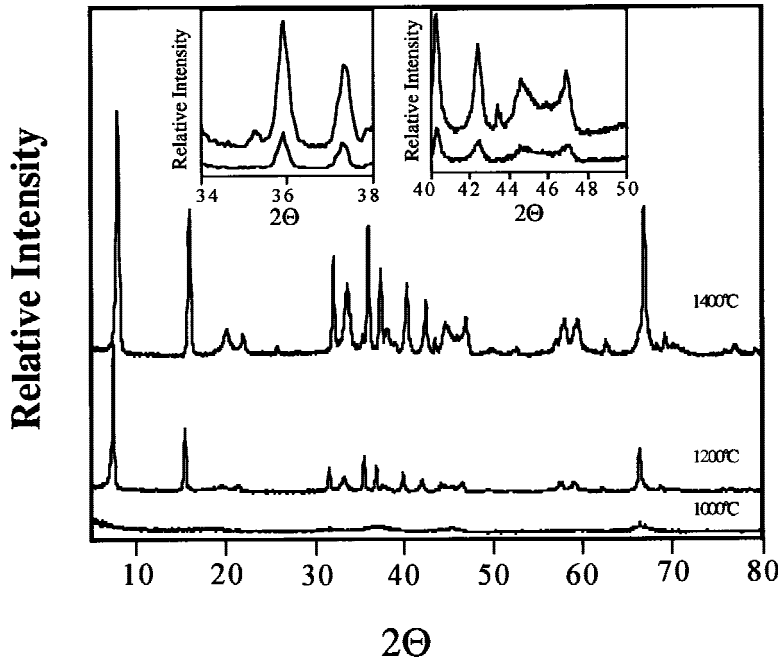

Fig. 4. XRD patterns of precursor 1 after bulk pyrolysis at 1000°C for 2 h, 1200°C for 2 h, and 1400°C for 1 h. Inset graphs shows expanded regions for the 1100°C (lower) and 1400°C (upper) XRD patterns; the strongest characteristic peak of β″-alumina (34.5°) is absent in each pattern, indicating pure β-alumina.

may indicate the presence of γ-alumina or other transition-alumina phases that share these particular reflections. Some extent of phase separation is implied, although it is also possible that the unique combination of rapid pyrolysis and cooling results in a metastable phase related to β″-alumina. Strikingly absent is any indication of the β-alumina phase, which has distinguishing diffraction peaks at 20.0° 2θ (4.45 Å), 21.8° 2θ (4.07 Å), and 33.5° 2θ (2.68 Å).

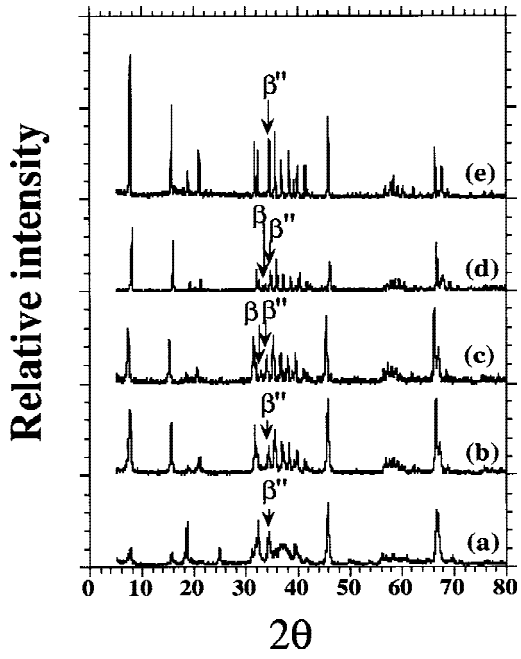

Fig. 5. XRD patterns of the nanopowder after various heat treatments (as-prepared (pattern (a)), 1200°C/1 h (pattern (b)), 1400°C/1 h (pattern (c)), and 1600°C/immediate cooling (pattern (d))); the XRD pattern of 100% crushed β″-alumina from a formed ceramic tube provided by Ceramatec is also shown (pattern (e)). Positions of the characteristic peaks from β- (33.5°) and β″-alumina (34.5°) are highlighted.

The XRD analysis of the nanopowder remains unchanged on heating to either 800°C for 1 h or 1000°C for 1 h. Heating to 1200°C for 1 h causes a change to occur (pattern (b) in Fig. 5). The 003 and 006 peaks at 7.66° 2θ (11.5 Å) and 15.6° 2θ (5. 69 Å), respectively, exhibit increased intensity, and all the unassigned peaks disappear. Peaks due to β-alumina remain absent. Thus, the observed pattern can be unambiguously assigned to phase-pure β″-alumina (the powder XRD pattern of a crushed β″-alumina sample from Ceramatec is given as pattern (e) in Fig. 5).

Because the more-traditional (and thermodynamically driven) bulk pyrolysis of the polymeric precursor yields only the β-phase, the rapid pyrolysis of the flame spray approach provides a unique mechanistic alternative, resulting in β″-alumina. There are clear kinetic advantages to the flame spray approach. Specifically, the rapid cooling following pyrolysis retards Na_2O volatilization, which helps to maintain the proper β″-alumina stoichiometry. This feature is not sufficient, however, because a similar effect could be achieved via bulk pyrolysis of the precursor at temperatures below the sublimation temperature of Na_2O (1275°C). As noted above, precursor pyrolysis at 1100°C resulted in β-alumina only. Another kinetic advantage of flame spray pyrolysis is that the precursor is heated to ~2000°C almost instantaneously. Essentially, the metal ions are blasted free of the organic matrix simultaneously, and, therefore, additional reactions to form the target oxide will not be limited by bulk diffusion, which leads to products that are almost as homogeneous as the original precursor.

The nanopowder begins to convert to the β-polytype on prolonged heating at 1400°C, as evidenced by the emergence of a signature peak at 33.5° 2θ (2.68 Å) (spectrum (c) in Fig. 5). The intensity of this peak increases on heating to 1600°C (immediate cooldown). As mentioned previously, both phases form over a range of sodium contents, although β-alumina does have the greater stability when the sodium amount is low. The conversion of β″-alumina to β-alumina at 1400°C is likely related to sodium loss through volatilization of Na_2O. Addi-

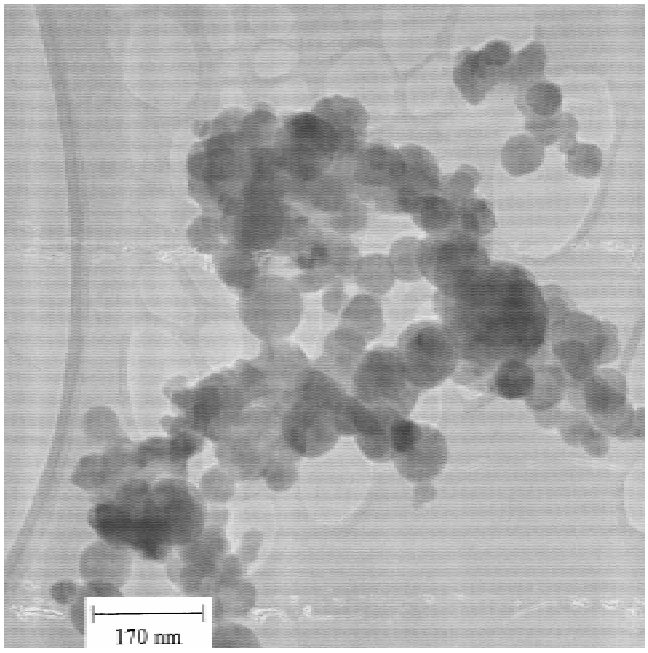

Fig. 6. TEM micrograph of the nanopowder from the pyrolysis of precursor 1; the top edge of the scale box represents 170 nm.

tional heating to 1600°C increases the volatilization and, hence, the amount of β″-alumina converted to β-alumina.

A TEM micrograph of as-prepared nanopowder is given in Fig. 6. As observed in the synthesis of other oxides,[14] the particle sizes range from 10 to 150 nm. The particle shapes are spherical with some faceting, which suggests limited crystallinity.

Thermal analysis of the nanopowder was performed using TGA and DTA experiments. TGA shows a small total mass loss of 2.4%, which occurs in two regions: one region centered at 100°C, where removal of surface bound moisture would be expected, and the second region centered at 800°C, where the decomposition of small amounts of carbonate contamination would likely occur.[18] No thermal events were observed in DTA analysis in the temperature range of 25°–1400°C. Given that a change in the XRD pattern of the nanopowder was observed after 1200°C, the absence of thermal events in the DTA indicates either a transformation of very low energy (i.e., additional crystallization of β″-alumina) or one that is augmented by the high surface energy of the nanopowders.

DRIFTS spectra of the nanopowders were taken on as-formed material and after treatment at 1200°C. The untreated powder possesses a broad, overlapping manifold of strong peaks from 500 to 1050 cm^{-1}. After heating to 1200°C, where the crystallization of β″-alumina is clear, more well-defined peaks appear at 620, 670, 740, and 800 cm^{-1}. These compare favorably (although not exactly) with those observed when the Ceramatec precursor powder is heated to 1200°C (converting to ~1:1 β:β″). The spectra also have a small broad peak in the ν(OH) region (~3500 cm^{-1}); its weak intensity suggests a small amount of surface hydroxyl groups from chemisorbed water.

Flame spray pyrolysis of precursors 2 and 3 results in nanopowders with slightly different behavior. The XRD pattern of as-pyrolyzed precursor 2 is almost amorphous, whereas that of precursor 3 shows only moderately more crystallinity (spectrum a in Figs. 7(a) and (b), respectively). As with the type 1 nanopowder, the X-ray patterns begin to change at 1200°C (see spectrum b in Figs. 7(a) and (b)). Although the observed peaks correspond to β″-alumina (with no clear peaks from β-alumina), the phases are much-less crystalline than those originally observed for precursor 1. Heating nanopowders of precursors 2 and 3 to 1400°C (12 min dwell time) increases their crystallinity; however, the higher temperature risks Na_2O volatilization and the accompanying β″-to-β conversion. The short isotherms used here may retard Na_2O loss, because nanopowder 2 has no noticeable β-alumina peaks. Nanopowder 3 does not have a clear β-alumina peak at 32.5° 2θ; however, a high background in that region may indicate that it is beginning to form.

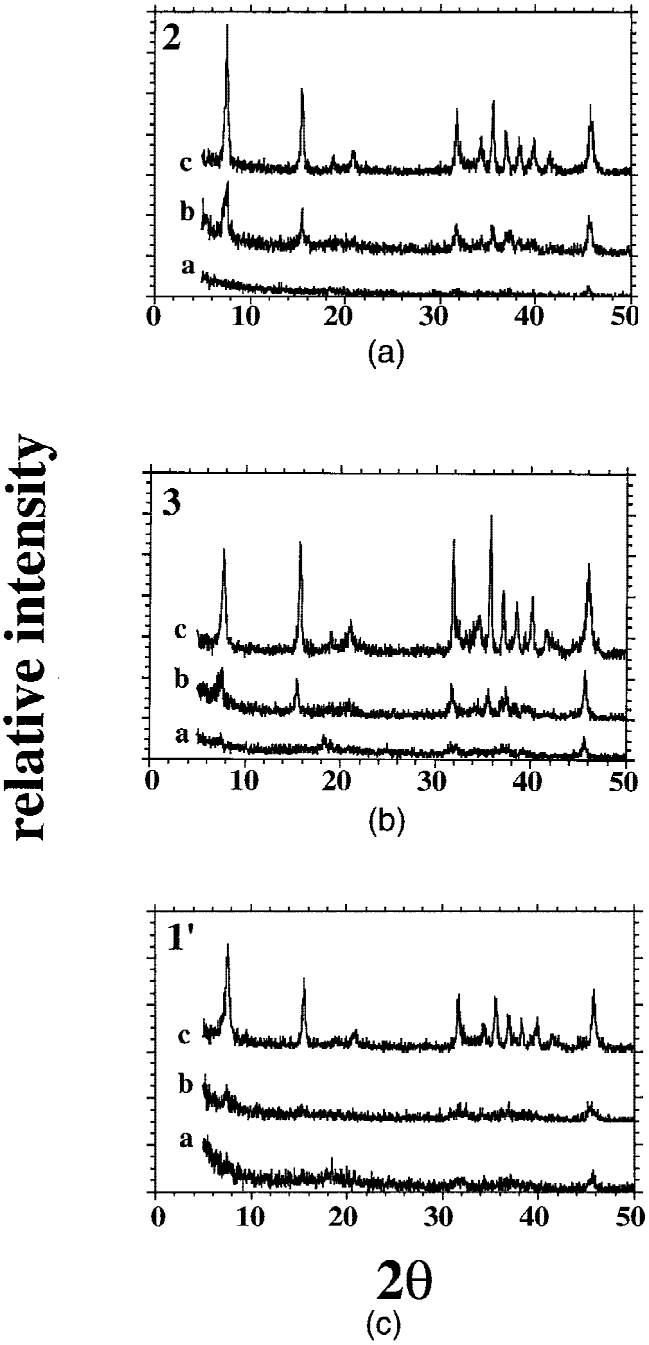

Fig. 7. XRD patterns of nanopowders from the pyrolysis of precursors (a) 2, (b) 3, and (c) 1′ (as-prepared (pattern a), 1200°C/1 h (pattern b), and 1400°C/12 min (pattern c).

Nanopowder from the pyrolysis of different batches of precursor 1 (designated 1′) behaves similarly to nanopowders 2 and 3. Fresh batches of nanopowder 1′ are almost amorphous (spectrum a in Fig. 7(c)), with weak crystalline peaks appearing at 1200°C (spectrum b in Fig. 7(c)). At 1400°C, β″-alumina is clearly observed whereas β-alumina is not (spectrum c in Fig.

7(c)). These changes in nanopowder behavior may be due to variations in the flame-spray-pyrolysis process. The actual pyrolysis temperature is not strictly controlled and can vary with such parameters as precursor concentration and gas flow rates. It is possible that the subsequent precursors were pyrolyzed at a lower temperature than that achieved in the original pyrolysis of precursor 1; therefore, the resulting nanopowders behave somewhat differently. Fortunately, these variations do not alter the eventual conversion to β″-alumina, which remains consistent from batch to batch of precursor 1 and with the slight changes in metal content of precursors 2 and 3.

(3) Nanopowder Sintering

The synthesis of high-purity β″-alumina is significant but cannot stand alone. These nanopowders must also be processed into dense ceramic shapes. Preliminary studies have been undertaken (using nanopowder from precursor 1) to demonstrate the potential to fabricate shapes and to identify some of the optimal parameters for sintering and densification.

Figure 8(a) is a plot of sintered-disk density with variation in several processing parameters. The compact densities remain essentially unchanged after sintering to 1200°C for 1 h. On heating to 1600°C (followed by immediate cooling), all disks show sharp increases in density. The highest value (2.81 ± 0.11 g/cm^3) is for the disk formed at the highest compaction pressure (52 ksi (~350 MPa)) with no binder used. These samples also exhibit a high degree of end capping after sintering. This observation is expected, because the high compaction pressure is applied uniaxially; therefore, the resulting disks have large density gradients. Additional exploration of the effects of compaction pressure on these bodies will be done using cold isostatic pressing (CIP), where the pressure is applied hydrostatically.

Similar experiments were performed on disks composed of nanopowder, using 20 wt% $Na_{1.67}Al_{10.67}Li_{0.33}(TEA)_{10.67}$-(EG)·$x$EG as a binder to enhance processability and sintered densities. The resulting compacts were somewhat easier to handle (better green compact mechanical properties). The use of binder with a compaction pressure of 25 ksi provided a noticeable increase in sintered density over compacts where no binder was used. No improvements were observed at higher compaction pressures; the sintered densities with and without binder were within error of each other.

Figure 8(b) plots disk density as a function of the isotherm duration (length) at 1600°C. The disks were formed from nanopowder alone at 25 ksi. The highest densities obtained were 3.1 g/cm^3, with an average of 3.0 ± 0.1 g/cm^3, which is 92% of the theoretical density for β″-alumina (3.26 g/cm^3).[23] Densities reached a maximum after 12 min of heating and did not increase with longer isotherms. To be useful in electrochemical devices, nonporous bodies with densities of ≥98% must be achieved. The processing techniques investigated so far have been the simplest at hand; other techniques may be more amenable to forming dense bodies from the nanopowders. Also, the high homogeneity of the nanopowders may

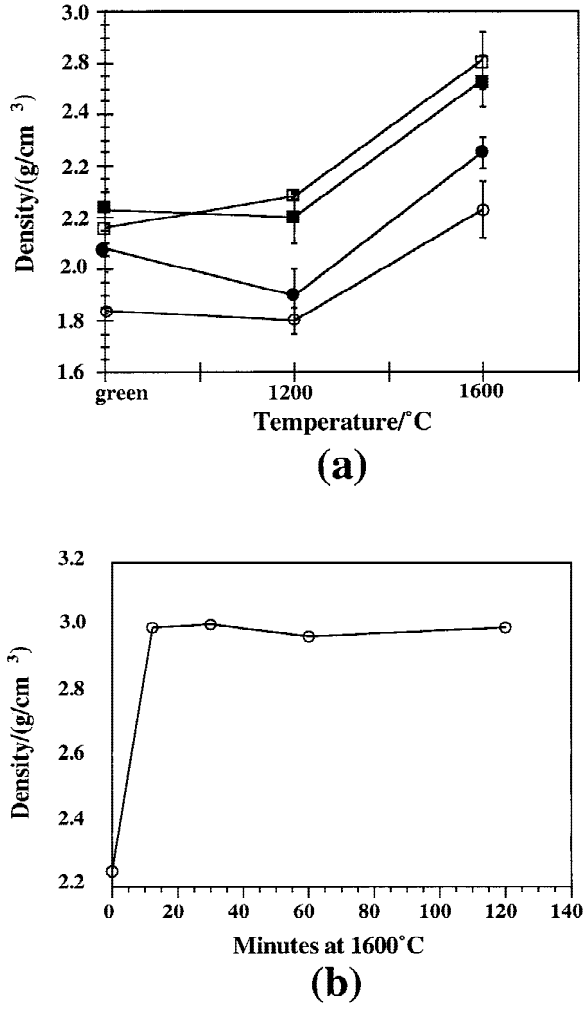

Fig. 8. (a) Sintered densities of compacted pellets of nanopowder from precursor 1, as a function of temperature (1200°C/1 h and 1600°C/immediate cooling) (compacts made (○) without binder at 25 ksi pressure, (●) with binder at 25 ksi pressure, (□) without binder at 51 ksi pressure, and (■) with binder at 52 ksi pressure). (b) Sintered densities of compacted pellets of nanopowder, as a function of the duration (length) of isotherm; the pellets were formed without binder at a pressure of 25 ksi applied uniaxially.

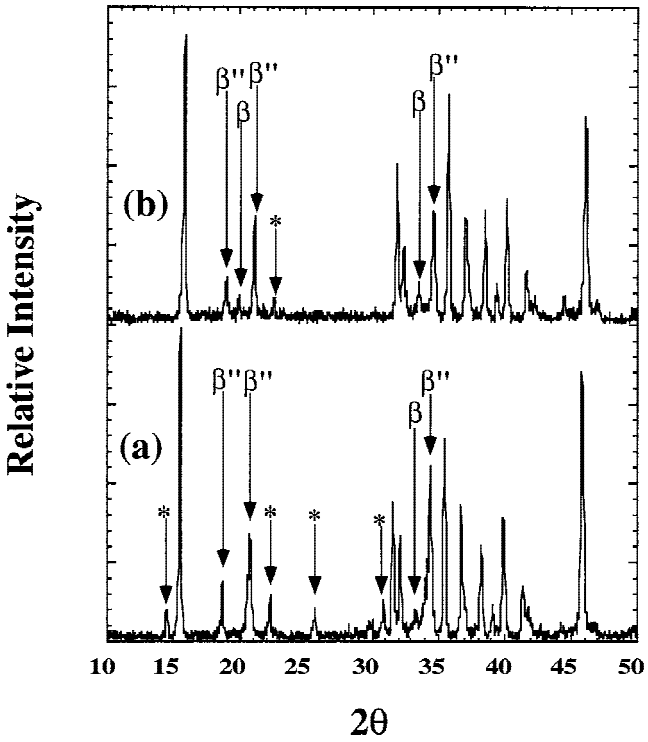

Fig. 9. XRD patterns of a compacted pellet of nanopowder after sintering at 1600°C (no dwell time) (the face of the intact pellet (pattern (a)) and fragments of the pellet ground to a powder (pattern (b))). Peaks characteristics of β- and β″-alumina are marked, as well as peaks that are of unknown origin (denoted by "*").

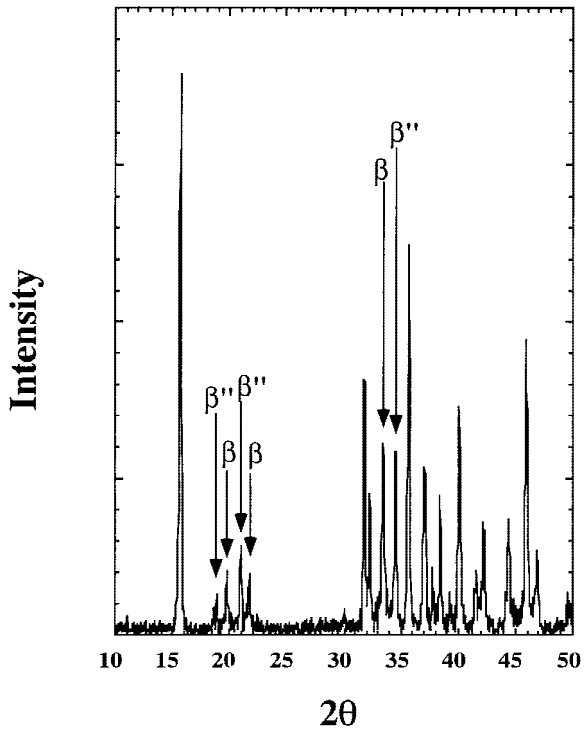

Fig. 10. XRD pattern of a compacted pellet of Ceramatec precursor powder after sintering at 1600°C (no dwell time).

partly limit subsequent densification, because inhomogeneities and impurities can lead to intermediate glassy phases that aid in sintering. This problem could be addressed by the controlled introduction of dopants and binders into the fabrication process.

The sintering behavior explored to date still results in β″-alumina as the dominant phase. A typical XRD pattern of a sintered compact is shown in Fig. 9. A small amount of β-alumina appears in bodies sintered to 1600°C, which indicates that additional measures to prevent Na_2O volatilization are needed (i.e., enclosing the bodies in platinum foil). Several other unknown peaks are also present. These are most likely due to surface impurities, because when the interior of the pellets are exposed by grinding, they largely disappear (spectrum (a) in Fig. 9). Some of the unknown peaks may originate from several possible alkali aluminates, although no one phase accounts for all of them.

For comparison purposes, disks were formed from as-received β″-alumina precursor powder provided by Ceramatec. The green compacts are amorphous; Fig. 10 shows a typical diffraction pattern after sintering to 1600°C (no dwell time). None of the surface impurities observed in the sintered nanopowders are present in the Ceramatec samples; however, these bodies are only ~50% β″-alumina via XRD. Formation of phase-pure β″-alumina from the Ceramatec precursor is certainly very sensitive to the heating schedule that is used. This condition makes the nanopowders a significant improvement, in that high-purity β″-alumina can be easily synthesized without rigorous, and possibly temperamental, processing protocols. Also, the densities of the Ceramatec compacts are in the range of 2.9–3.0 g/cm^3—comparable to those achieved with the nanopowder under the same processing conditions. This similarity emphasizes that more-sophisticated processing techniques are required in both systems to achieve the desired densities of ≥98%.

The question of nanopowder stability, with respect to reproducible formation of β″-alumina, is important. Many of the processing steps explored thus far have not been executed with rigorous regard to purity (i.e., preparations are performed in air with undistilled solvents). Still, high-purity β″-alumina is produced consistently. Nanopowders left exposed to the atmosphere for several days (25°–50°C) prior to sintering give identical results. Although more-rigorous efforts to prevent Na_2O volatilization during sintering are required, the nanopowder stability toward the atmosphere simplifies many handling procedures.

Figures 11 and 12 show various views of the sintered compacts formed from nanopowder and Ceramatec precursor powder, respectively. The Ceramatec compacts have rodlike grains (0.2 × 1.0 μm) on both the pellet surface and the exposed fracture surface. The fracture surface of the nanopowder compacts is similar, exhibiting platelike (0.3 × 0.3 μm) or rodlike (0.3 × 1.0 μm) grains of comparable size. These grains seem slightly more crystalline than those of the Ceramatec compacts; that is, the edges and facets of the grains appear smoother and straighter. However, the appearance of the grains on the disk surface differs; here, slightly larger (1–2 μm) polyhedral grains

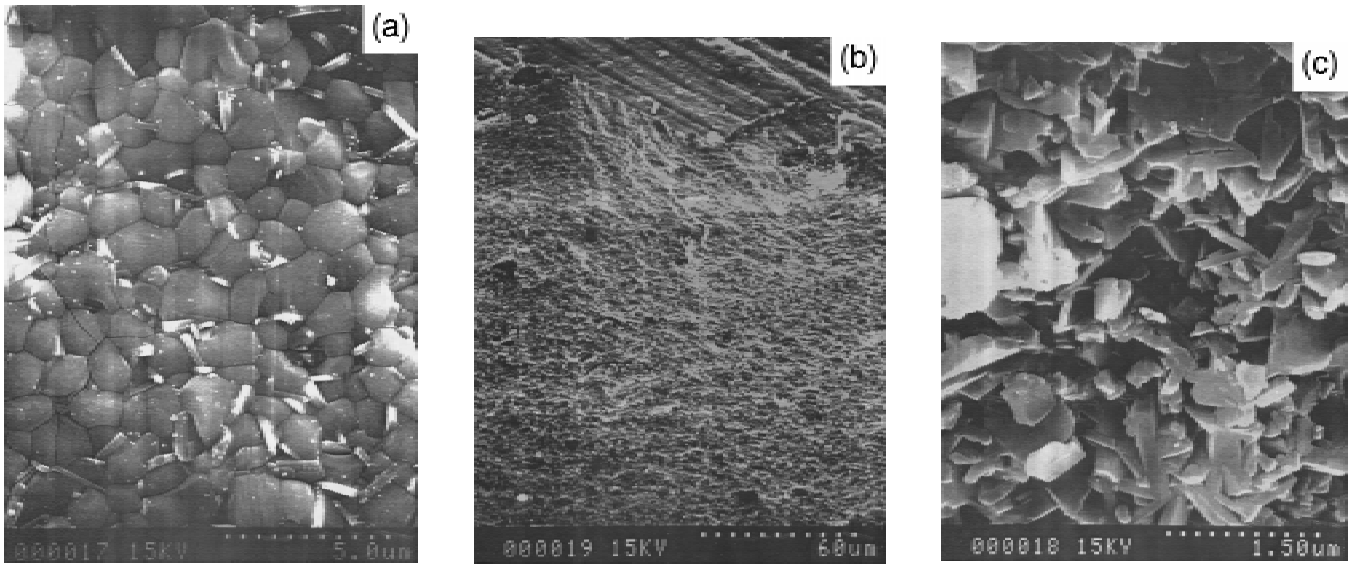

Fig. 11. SEM micrographs of a compacted pellet of nanopowder after sintering at 1600°C (no dwell time) ((a) view of the top of the pellet, (b) low-magnification view of the fracture edge, and (c) high-magnification view of the fracture edge).

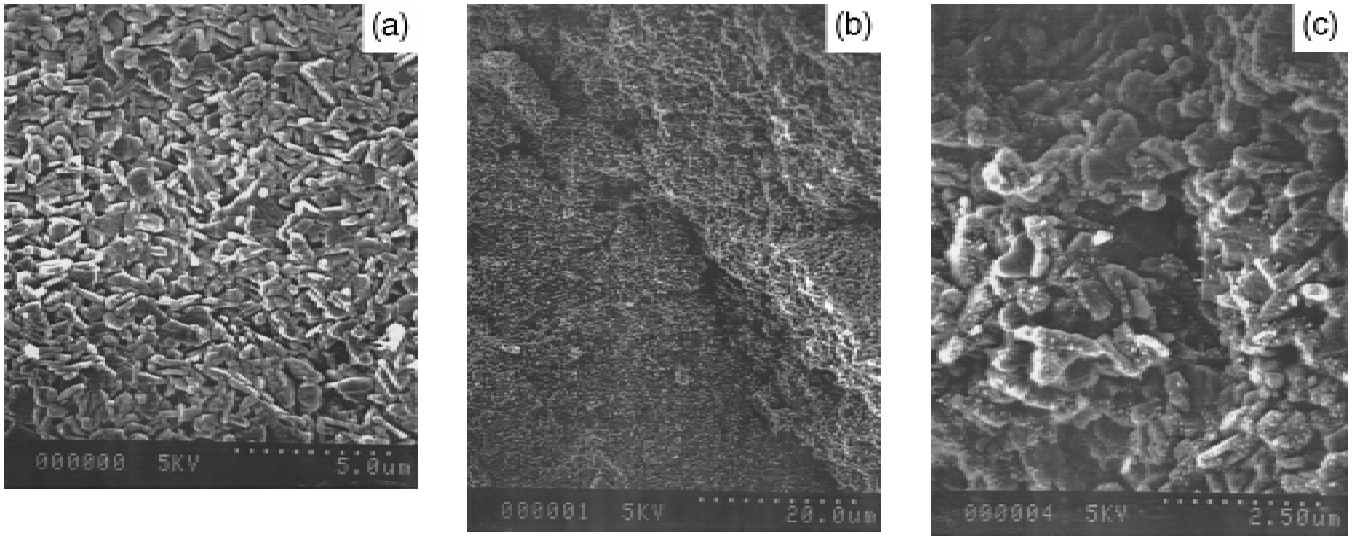

Fig. 12. SEM micrographs of a compacted pellet of Ceramatec precursor after sintering at 1600°C (no dwell time) ((a) view of the top of the pellet, (b) low-magnification view of the fracture edge, and (c) high-magnification view of the fracture edge).

have grown to abut each other tightly. The modified surface grains may be related to the unknown diffraction peaks noted in the XRD pattern of the pellet surface.

IV. Summary and Conclusions

Flame spray pyrolysis of polymer-like precursors results in high-purity lithium-doped β″-alumina. Large quantities of the nanopowder intermediate (100 g/h)[14] are accessible from inexpensive and easily handled starting materials. Initial indications are that the nanopowders can be processed successfully into dense, almost-pure-phase ceramic monoliths. The undesired polytype, β-alumina, is totally avoided until the nanopowders are subjected to temperatures above the sublimation temperature of Na_2O. The rapid heating and cooling of the reactants, which occurs in flame spray pyrolysis, apparently provides access to a different reaction pathway which favors the formation of the β″-alumina. In the future, it may be possible to exploit this feature in the synthesis of other complex oxides.

Acknowledgments: The authors wish to thank the following individuals for their assistance: Rita Baranawal and Tom Hinklin, for nanopowder pyrolysis; Ram Narayanan, for NMR spectroscopy; Mark Nechanicky, for the TEM analyses; and Yin Liu, for the SEM analyses.

References

[1]Y.-F. Y. Yao and J. T. Kummer, ''Ion Exchange Properties of and Rates of Ionic Diffusion in Beta-Alumina,'' *J. Inorg. Nucl. Chem.*, **29**, 2453–75 (1967).

[2](a) W. J. Walsh, ''Advanced Batteries for Electric Vehicles—A Look at the Future,'' *Phys. Today*, **33** [6] 34–41 (1980). (b) J. L. Sudworth and A. R. Tilley (eds.), *The Sodium Sulfur Battery*. Chapman and Hall, London, U.K., and New York, 1985.

[3](a) J. T. Kummer and N. Weber, ''Energy Conversion Device Comprising a Solid Crystalline Electrolyte and a Solid Reaction Zone Separator,'' U.S. Pat. No. 3 404 036, 1986. (b) N. Weber, ''A Thermoelectric Device Based on Beta-Alumina Solid Electrolyte,'' *Energy Convers.*, **14**, 1–9 (1974). (c) T. Cole, ''Thermoelectric Energy Conversion with Solid Electrolytes,'' *Science*, **221**, 915–20 (1983).

[4](a) B. M. Kulwicki, ''Ceramic Sensors and Transducers,'' *J. Phys. Chem.*, **45**, 1015–31 (1984). (b) A. Jones, P. Moseley, and B. Tofield, ''The Chemistry of Solid State Gas Sensors,'' *Chem. Br.*, **23**, 749–54 (1987). (c) H. Näfe, ''The Feasibility of a Potentiometric CO_2 Sensor Based on Na-Beta-Alumina in the Light of the Electronic Conductivity of the Electrolyte,'' *Sens. Actuators B*, **21**, 79–86 (1994).

[5] (a) J. T. Kummer, ''β-Alumina Electrolytes,'' *Prog. Solid State Chem.*, **7**, 141–75 (1972). (b) B. Dunn and G. C. Farrington, ''Fast Divalent Ion Conduction in Ba^{++}, Cd^{++}, and Sr^{++} Beta″-Alumina,'' *Mater. Res. Bull.*, **15**, 1773–77 (1980). (c) G. C. Farrington and B. Dunn, ''Divalent Beta″-Alumina: High Conductivity Solid Electrolytes for Divalent Cations,'' *Solid State Ionics*, **7**, 267–81 (1982). (d) S. Sattar, B. Ghosal, M. L. Underwood, H. Mertwoy, M. A. Saltzberg, W. S. Frydrych, G. S. Rohrer, and G. C. Farrington, ''Synthesis of Di- and Trivalent β″ Aluminas by Ion Exchange,'' *J. Solid State Chem.*, **65**, 231–40 (1986).

[6]B. Dunn and G. C. Farrington, ''Recent Developments in β″ Alumina,'' *Solid State Ionics*, **18/19**, 31–39 (1986).

[7](a) G. C. Farrington, B. Dunn, and J. O. Thomas, ''The Lanthanide β″ Aluminas: A New Family of Fluorescent Solid Electrolytes,'' *Appl. Phys. A*, **A32**, 159–61 (1983). (b) B. Dunn, G. C. Farrington, and J. O. Thomas, ''Frontiers in β″-Alumina Research,'' *MRS Bull.*, **14** [9] 22–30 (1989).

[8](a) G. Yamaguchi and K. Suzuki, ''On the Structures of Alkali Polyaluminates,'' *Bull. Chem. Soc. Jpn.*, **41**, 93–99 (1968). (b) R. Stevens and J. P. G. Binner, ''Review: Structure, Properties, and Production of β-Alumina,'' *J. Mater. Sci.*, **19**, 695–715 (1984). (c) M. Bettman and C. R. Peters, ''The Crystal Structure of $Na_2O{\cdot}MgO{\cdot}5Al_2O_3$ with Reference to $Na_2O{\cdot}5Al_2O_3$,'' *J. Phys. Chem.*, **73**, 1774–80 (1969).

[9]R. C. DeVries and W. L. Roth, ''Critical Evaluation of the Literature Data on Beta Alumina and Related Phases: I, Phase Equilibria and Characterization of Beta Alumina Phases,'' *J. Am. Ceram. Soc.*, **52**, 364–69 (1969).

[10](a) G. J. May and S. R. Tan, ''Recent Progress in the Development of Beta-Alumina for the Sodium-Sulfur Battery,'' *Electrochim. Acta*, **24**, 755–63 (1979). (b) A. V. Virkar, G. R. Miller, and R. S. Gordon, ''Resistivity–Microstructure Relations in Lithia-Stabilized Polycrystalline β″-Alumina,'' *J. Am. Ceram. Soc.*, **61**, 250–52 (1978). (c) A. Imai and M. Harata, ''Ionic Conduction of Impurity-Doped β-Alumina Ceramics,'' *Jpn. J. Appl. Phys.*, **11**, 180–85 (1972).

[11](a) R. Hartung, ''Process for the Preparation of an Ion-Conduction Ceramic Material,'' U.S. Pat. No. 5 232 681, 1993. (b) P. E. D. Morgan, ''Preparation of Powders Suitable for Conversion to Useful Beta-Aluminas,'' U.S. Pat. No. 4 339 511, 1982. (c) D. S. Eddy and J. F. Rhodes, ''Method of Making Sodium Beta-Alumina Powder and Sintered Articles,'' U.S. Pat. No. 4 052 538, 1977. (d) A. Van Zyl, G. K. Duncan, P. Barrow, and M. Thackeray, ''Method of Making Beta″-Alumina,'' U.S. Pat. No. 4 496 664, 1990. (e) A. Van Zyl, M. M. Thackeray, G. K. Duncan, A. I. Kingon, and R. O. Heckroodt, ''The Synthesis of Beta Alumina from Aluminum Hydroxide and Oxyhydroxide Precursors,'' *MRS Bull.*, **28**, 145–57 (1993). (f) D. W. Johnson, S. M. Granstaff, and W. W. Rhodes, ''Preparation of β″-Al_2O_3 Pressing Powders by Spray Drying,'' *Am. Ceram. Soc. Bull.*, **58**, 849–52 (1979). (g) M. L. Miller, B. J. McEntire, G. R. Miller, and R. S. Gordon, ''A Prepilot Process for the Fabrication of Polycrystalline β″-Alumina Electrolyte Tubing,'' *Am. Ceram. Soc. Bull.*, **58**, 522–24 (1979).

[12]R. C. Weast (ed.), *Handbook of Chemistry and Physics, 66th Ed.*; p. B-144. CRC Press, Boca Raton, FL, 1985.

[13]R. M. Laine, D. R. Treadwell, B. L. Mueller, C. R. Bickmore, K. F. Waldner, and T. Hinklin, ''Processable Aluminosilicate Alkoxide Precursors from Metal Oxides and Hydroxides. The Oxide One Pot Synthesis (OOPS) Process,'' *J. Chem. Mater.*, **6** [8] 1441–43 (1996).

[14]C. R. Bickmore, K. F. Waldner, D. R. Treadwell, and R. M. Laine, ''Ultrafine Spinel Powders by Flame Spray Pyrolysis of a Magnesium Aluminum Double Alkoxide'' *J. Am. Ceram. Soc.*, **79**, 1419–23 (1996).

[15](a) H. Gleiter, ''Materials with Ultrafine Microstructures: Retrospectives and Perspectives,'' *Nanostruct. Mater.*, **1**, 1–19 (1992). (b) G. D. Ulrich, ''Flame Synthesis of Fine Particles,'' *Chem. Eng. News*, **62** [32] 22–29 (1984).

[16]A. C. Sutorik, S. S. Neo, and R. M. Laine; work in progress.

[17]Y. Liu, Z.-F. Zhang, B. King, J. Halloran, and R. M. Laine. ''Synthesis of Yttrium Aluminum Garnet Using Isobutyrate Precursors,'' *J. Am. Ceram. Soc.*, **76**, 385–94 (1996).

[18]P. Kansal and R. M. Laine, ''Group II Tris(glycolato)silicates as Precursors to Silicate Glasses and Ceramics'' *J. Am. Ceram. Soc.*, **78**, 529–38 (1995).

[19]R. Baranwal and R. M. Laine, ''A Preceramic Polymer Route to Amorphous and Crystalline Potassium Aluminosilicate Powders and Their Electrorheological Properties,'' *J. Am. Ceram. Soc.*, **80** [6] 1436–46 (1997).

[20]J. Pinkas and J. Verkade, ''Alumatrane, $Al(OCH_2CH_2)_3N$: A Reinvestigation of Its Oligomeric Behavior,'' *Inorg. Chem.*, **32**, 2711–16 (1993).

[21]K. F. Waldner, R. M. Laine, S. Dhumrongvaraporn, S. Tayaniphan, and R. Narayanan, ''Synthesis of a Double Alkoxide Precursor to Spinel ($MgAl_2O_4$) Directly from $Al(OH)_3$ MgO, and Triethanolamine, and its Pyrolytic Transformation to Spinel,'' *Chem. Mater.*, **8**, 2850–57 (1996).

[22]J. D. Hodge, ''Powder Processing and Crystalization of Beta and Beta″ Aluminas,'' *Am. Ceram. Soc. Bull.*, **62**, 244–48 (1983).

[23]G. E. Youngblood, A. V. Virkar, W. R. Cannon, and R. S. Gordon, ''Sintering Processes and Heat Treatment Schedules for Conductive, Lithia-Stabilized β″-Al_2O_3,'' *Am. Ceram. Soc. Bull.*, **56**, 206–10 (1977). □